

## FROM LIGHT-CURVES TO FREQUENCIES OF OSCILLATION MODES USING TACO

N. Themeßl<sup>1,2</sup>, J. S. Kuzlewicz<sup>1,2</sup>, A. García Saravia Ortiz de Montellano<sup>1,2</sup> and S. Hekker<sup>1,2</sup>

**Abstract.** The TACO code (**T**ools for **A**utomated **C**haracterization of **O**scillations) has been developed to provide an automated, fast and reliable analysis of solar-like oscillations. We demonstrated its capabilities, based on the asteroseismic study of an open-cluster red giant that has been observed by the *Kepler* space mission. TACO uses as input a light-curve corrected for systematics, and after several analysis steps it provides the characteristics of all statistically-significant oscillation modes, including mode identification.

Keywords: Asteroseismology, Methods: data analysis, Stars: individual: KIC 4937257, Stars: oscillations

### 1 Introduction

State-of-the-art space missions such as *CoRoT*, *Kepler*, *K2* and *TESS* (e.g., Baglin et al. 2006; Borucki et al. 2010; Howell et al. 2014; Ricker et al. 2015), have been – and are still – providing high-precision photometric light-curves for an unprecedented number of oscillating stars, and with more data coming (e.g., *TESS* extended mission and *PLATO* Rauer et al. 2014). In the case of solar-like oscillations, the modes form a distinctive pattern in the observed frequency spectrum of the star. Several radial orders of low spherical degree modes ( $\ell \leq 3$ ) can be detected; those are suitable for automated procedures to extract their characteristics in the tens of thousands of stars that show solar-like oscillations. General attempts to detect these oscillation frequencies are based on the asymptotic relation (Tassoul 1980), or the so-called “universal pattern” (Mosser et al. 2011). These approaches can be hampered if mode frequencies are below the detection limit; they need careful inspection on a mode-by-mode basis, and are prone to a certain degree of subjectivity.

In order to handle the large number of stars for which we have data, we introduced the TACO code, which consists of a sequence of modules that perform an analysis of solar-like oscillations. We have implemented a data-driven Mexican-hat wavelet-transform based a detection method to search for all the statistically-significant peaks in the observed frequency spectrum (?). This algorithm is appropriate for detecting peaks that are approximately symmetric, have a positive peak height, and a finite width, as is the case for solar-like oscillation modes. Commonly used astrophysical concepts are only included in other parts of the analysis; more information will be available in the main TACO paper, which will be submitted soon. The final output is a list of frequencies and mode identifications of the oscillations. As a byproduct, TACO provides some of the global oscillation parameters, among which are the frequency of maximum oscillation power ( $\nu_{\max}$ ), the large and small frequency separations, the period spacing and the coupling factor, and also the rotational splitting (if present).

### 2 Characterization of solar-like oscillations using TACO

Here we present the analysis of the oscillating red-giant star KIC 4937257, which is a member of the open cluster NGC 6819. We focus on two of the modules that are implemented in TACO; they involve background fitting of power density spectra (PDS), including  $\nu_{\max}$  estimation and automated detection of peaks in the observed frequency range of the oscillations. As a general input, TACO uses light-curve data. Those are first high-pass filtered (default = 40 days), and we then compute a PDS from the filtered light-curve normalized by the window function (see Fig. 1). Next, we obtain estimates of the location of the oscillation power excess, i.e.  $\nu_{\max}$ , from the variance of the photometric time-series and the application of both the Morlet and the Mexican-Hat wavelets to the PDS. A comparison between these three estimates provides a preliminary value of  $\nu_{\max}$ , which will be used to set some priors for subsequently fitting a global model to the PDS. For more information on these modules we refer the interested reader to the main TACO paper.

---

<sup>1</sup> Max Planck Institute for Solar System Research, Justus-von-Liebig-Weg 3, DE-37077 Göttingen, Germany

<sup>2</sup> Stellar Astrophysics Centre (SAC), Department of Physics and Astronomy, Aarhus University, Ny Munkegade 120, DK-8000 Aarhus C, Denmark

### 2.1 Global background model fit and determination of $\nu_{\max}$

The next step uses a global fit to estimate the granulation and white noise background level on which the oscillation modes lie. By default, TACO applies a model to the PDS that consists of a Gaussian function to approximate the oscillation power envelope, three granulation background components, and a single parameter to account for the white noise in the data (Fig. 1; for functional forms of the model, see the main TACO paper). To reduce the computation time during the background fitting process, TACO uses a binned version of the PDS with a default set to 300 bins ( $\approx 0.94 \mu\text{Hz}$ -wide bins). By basing this on a Bayesian Markov Chain Monte Carlo (MCMC) framework with affine-invariant ensemble sampling (EMCEE; Foreman-Mackey et al. 2013), we obtain posterior probability distributions for the fitted parameters and adopt the medians of those distributions as estimates of the expectation values and their 16<sup>th</sup>/84<sup>th</sup> percentiles as uncertainties. In Figure 2 we show the results for the background fits based on different binnings and their influences on the estimates of  $\nu_{\max}$ .

The following arguments can be applied to optimize the output from this module: the number of walkers (chains) for the fit (default = 50), the number of steps for the MCMC warm-up (default = 1000), the minimum number of steps for the MCMC estimation (default = 2000), the maximum number of steps for the whole MCMC run (default = 5000) and the binning of the PDS for the fitting process\*.

### 2.2 Automated detection of significant peaks and mode identification

First, we divide the PDS by the background model which is comprised of the granulation and white noise components. A Mexican-hat wavelet-transform based algorithm then searches for the significant peaks in the predefined area of  $\nu_{\max} \pm 3$  times the width of the Gaussian function fitted to the oscillation power excess. Next, we optimize simultaneously the parameters of all the detected oscillation modes through maximum likelihood estimation, using a global model fit. From that fit, TACO provides a list of frequencies, amplitudes and linewidths. Those oscillation parameters are subsequently used for mode identification.

This part of the analysis can be applied iteratively in order to achieve an optimal result. For KIC 4937257, we first searched for the resolved peaks in the spectrum, which were then fitted with Lorentzian functions. We then used the mode identification module to detect the  $\ell = 0, 2$  modes in that preliminary list of frequencies by using well-established relations for solar-like oscillations (such as the “universal pattern”). We divided the PDS by a global model fit, including only the even modes, and reran the peak detection method. This time, we used TACO to detect both resolved and unresolved peaks, where the latter are fitted with sinc<sup>2</sup> functions. The final step was to combine the lists to obtain all the frequencies of statistically-significant oscillation modes. We have reported these results in Table 1. Figure 3 shows the different steps of the peak detections for KIC 4937257.

For the peak detection module, the optimization parameters are the minimum signal-to-noise ratio of the wavelet for resolved peaks (set to 1.3) plus the maximum search line-width for resolved peaks in the continuous wavelet transform (set to  $0.4 \mu\text{Hz}$ ) and the minimum (most frequent) probability threshold for unresolved peaks (default = 0.0001).

After obtaining the final list of frequencies, TACO evaluates the dipole modes ( $\ell = 1$ ), and a period spacing is estimated (if present). Finally, for the rotationally-split modes the azimuthal orders are identified and the rotational splitting is determined. A more detailed description of these remaining analysis modules can be found in our main TACO paper (in preparation).

## 3 Conclusions

With more asteroseismic data becoming available in the near future, TACO can provide an important step towards an automated and reliable asteroseismic study of solar-like oscillations in main-sequence, subgiant and red-giant stars. Owing to its modular design, each part of the analysis can be used separately and new modules can be included without much effort. For example, the module to detect significant peaks in a frequency spectrum could be very useful for extracting the observed frequencies of classical pulsators. TACO has been tested extensively on 4 years of *Kepler* data (i.e., APOKASC red-giant sample; Pinsonneault et al. 2014, 2018). In addition, we have successfully applied it to study the global oscillations of the Sun using BISON (García Saravia Ortiz de Montellano et al. 2018) and SPM Virgo data (Themeßl et al. in prep.), and also of  $\delta$  Eridani observed by the SONG network (Bellinger et al., in prep.), the subgiants  $\nu$  Indi (Chaplin et al., in press) and  $\beta$  Hydri observed by *TESS*.

---

\*To change the number of granulation components to two, substitute the class “KeplerBg3Comp” within the code to “KeplerBg2Comp”. Other functional forms of the fit can be implemented as new classes.

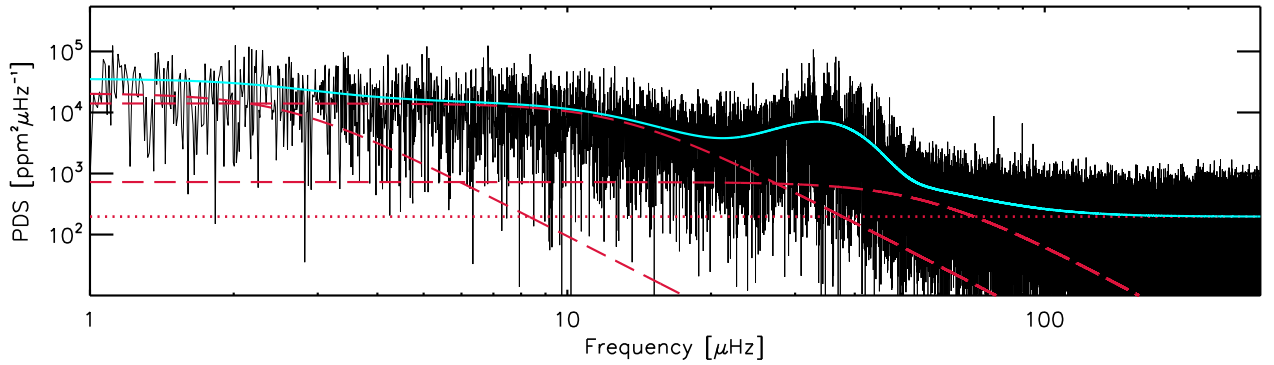


**Fig. 1.** Power density spectrum (in black) of KIC 4937257 showing our global model fit (in cyan), which comprises three granulation components (red dashed lines), one white noise component (horizontal red dotted line) and a Gaussian fit to the oscillation power excess.

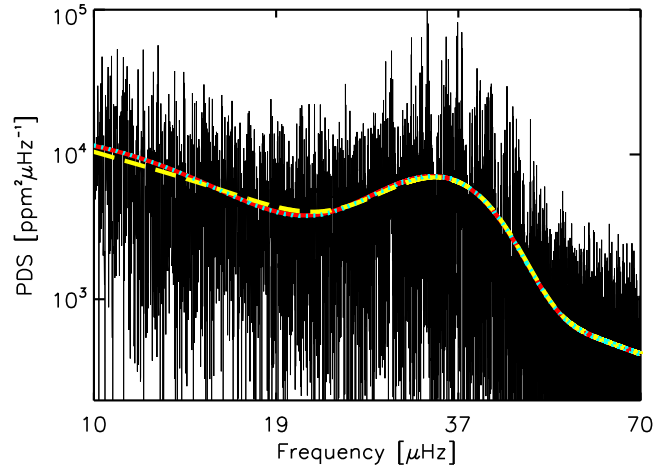


**Fig. 2.** Part of the power density spectrum of KIC 4937257 around the oscillation power excess is shown. The different colours represent the global fits based on different binnings. The  $\nu_{\max}$  estimates are:  $33.77 \pm 0.27 \mu\text{Hz}$  (300 bins, dotted red line),  $34.18 \pm 0.38 \mu\text{Hz}$  (50 bins, dashed yellow line) and  $33.79 \pm 0.26 \mu\text{Hz}$  (no binning of the data, dotted cyan line).

This work was funded by the European Research Council under the European Community's Seventh Framework Programme (FP7/2007-2013)/ERC grant agreement No. 338251 (StellarAges).

## References

- Baglin, A., Auvergne, M., Boisnard, L., et al. 2006, in 36th COSPAR Scientific Assembly, Vol. 36, 3749
- Borucki, W. J., Koch, D., Basri, G., et al. 2010, *Science*, 327, 977
- Foreman-Mackey, D., Hogg, D. W., Lang, D., & Goodman, J. 2013, *PASP*, 125, 306
- García Saravia Ortiz de Montellano, A., Hekker, S., & Themeßl, N. 2018, *MNRAS*, 476, 1470
- Howell, S. B., Sobeck, C., Haas, M., et al. 2014, *PASP*, 126, 398
- Mosser, B., Belkacem, K., Goupil, M. J., et al. 2011, *A&A*, 525, L9
- Pinsonneault, M. H., Elsworth, Y., Epstein, C., et al. 2014, *ApJS*, 215, 19
- Pinsonneault, M. H., Elsworth, Y. P., Tayar, J., et al. 2018, *ApJS*, 239, 32
- Rauer, H., Catala, C., Aerts, C., et al. 2014, *Experimental Astronomy*, 38, 249
- Ricker, G. R., Winn, J. N., Vanderspek, R., et al. 2015, *JATIS*, 1, 014003
- Tassoul, M. 1980, *ApJS*, 43, 469

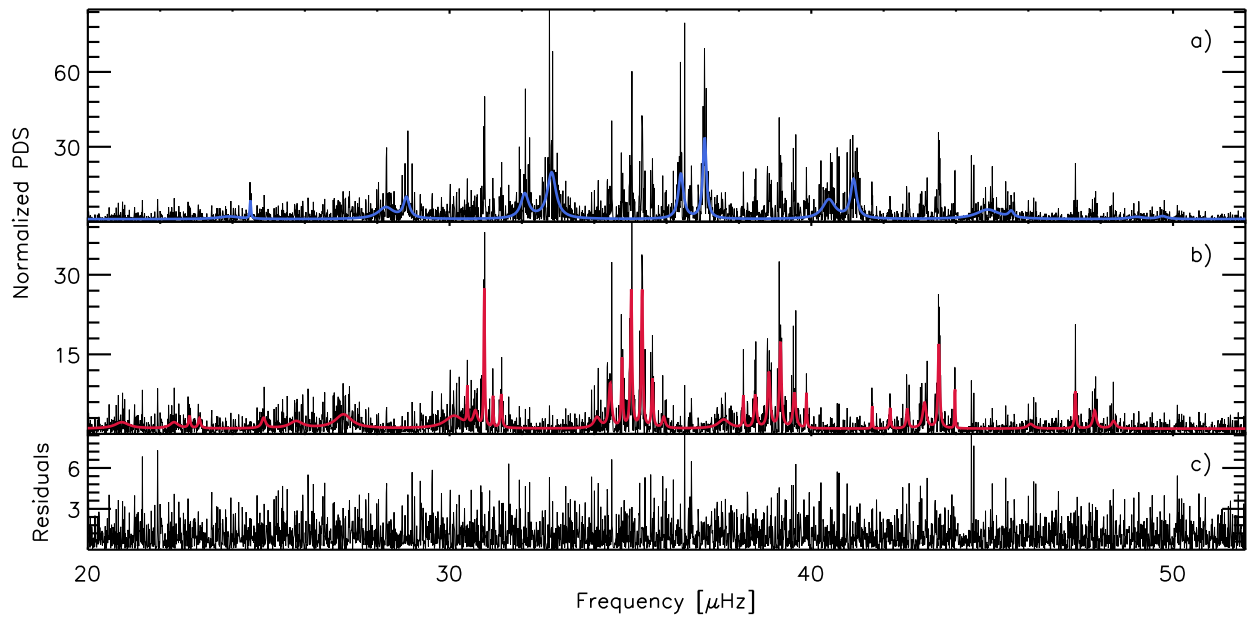


**Fig. 3.** Panel a): Background-normalized power density spectrum (PDS) covering the oscillation modes of the red giant, with a fit to the even modes (in blue). Panel b): PDS normalized by the global fit from panel a), now including the fit to the odd modes (in red); the residuals are shown in panel c).

**Table 1.** Characteristics of detected oscillation modes for KIC 4937257.

Frequency [ $\mu\text{Hz}$ ]	Amplitude	Linewidth [ $\mu\text{Hz}$ ]	Spherical degree
20.94 $\pm$ 0.08	0.94 $\pm$ 0.14	0.24 $\pm$ 0.12	1
22.38 $\pm$ 0.06	0.71 $\pm$ 0.14	0.14 $\pm$ 0.09	1
22.81 $\pm$ 0.02	0.45 $\pm$ 0.13	0.03 $\pm$ 0.02	1
23.08 $\pm$ 0.03	0.46 $\pm$ 0.12	0.04 $\pm$ 0.03	1
23.91 $\pm$ 0.13	1.13 $\pm$ 0.17	0.38 $\pm$ 0.16	2
24.49 $\pm$ 0.01	0.64 $\pm$ 0.14	0.02 $\pm$ 0.01	0
24.86 $\pm$ 0.03	0.63 $\pm$ 0.13	0.06 $\pm$ 0.04	1
25.76 $\pm$ 0.08	0.95 $\pm$ 0.15	0.22 $\pm$ 0.11	1
27.07 $\pm$ 0.06	1.51 $\pm$ 0.12	0.27 $\pm$ 0.06	1
28.24 $\pm$ 0.05	1.93 $\pm$ 0.20	0.26 $\pm$ 0.10	2
28.81 $\pm$ 0.03	1.59 $\pm$ 0.18	0.10 $\pm$ 0.04	0
30.12 $\pm$ 0.07	1.49 $\pm$ 0.14	0.30 $\pm$ 0.08	1
30.49 $\pm$ 0.01	0.56 $\pm$ 0.20	0.01 $\pm$ 0.01	1
30.71 $\pm$ 0.04	0.78 $\pm$ 0.19	0.07 $\pm$ 0.06	1
30.96 $\pm$ 0.01	1.14 $\pm$ 0.21	0.02 $\pm$ 0.01	1
31.20 $\pm$ 0.01	0.48 $\pm$ 0.15	0.01 $\pm$ 0.01	1
31.43 $\pm$ 0.01	0.70 $\pm$ 0.13	0.02 $\pm$ 0.01	1
32.08 $\pm$ 0.03	1.99 $\pm$ 0.18	0.13 $\pm$ 0.04	2
32.82 $\pm$ 0.02	2.90 $\pm$ 0.19	0.14 $\pm$ 0.03	0
34.08 $\pm$ 0.04	0.81 $\pm$ 0.14	0.10 $\pm$ 0.06	1
34.44 $\pm$ 0.02	1.11 $\pm$ 0.14	0.05 $\pm$ 0.02	1
34.77 $\pm$ 0.01	0.95 $\pm$ 0.16	0.02 $\pm$ 0.01	1
35.02 $\pm$ 0.01	1.44 $\pm$ 0.20	0.03 $\pm$ 0.01	1
35.32 $\pm$ 0.01	1.43 $\pm$ 0.20	0.02 $\pm$ 0.01	1
35.61 $\pm$ 0.01	0.85 $\pm$ 0.14	0.03 $\pm$ 0.01	1
35.92 $\pm$ 0.04	0.57 $\pm$ 0.13	0.05 $\pm$ 0.03	1
36.40 $\pm$ 0.02	2.19 $\pm$ 0.19	0.08 $\pm$ 0.02	2
37.05 $\pm$ 0.01	2.46 $\pm$ 0.23	0.06 $\pm$ 0.02	0
37.58 $\pm$ 0.06	0.99 $\pm$ 0.13	0.19 $\pm$ 0.08	3
38.12 $\pm$ 0.01	0.59 $\pm$ 0.15	0.02 $\pm$ 0.02	1
38.45 $\pm$ 0.02	0.86 $\pm$ 0.14	0.04 $\pm$ 0.02	1
38.83 $\pm$ 0.01	1.15 $\pm$ 0.15	0.04 $\pm$ 0.02	1
39.15 $\pm$ 0.01	1.28 $\pm$ 0.17	0.03 $\pm$ 0.01	1
39.53 $\pm$ 0.02	0.97 $\pm$ 0.13	0.05 $\pm$ 0.02	1
39.87 $\pm$ 0.01	0.55 $\pm$ 0.13	0.01 $\pm$ 0.01	1
40.48 $\pm$ 0.04	2.24 $\pm$ 0.16	0.21 $\pm$ 0.05	2
41.17 $\pm$ 0.02	2.17 $\pm$ 0.18	0.10 $\pm$ 0.02	0
41.68 $\pm$ 0.01	0.39 $\pm$ 0.11	0.01 $\pm$ 0.01	1
42.18 $\pm$ 0.01	0.47 $\pm$ 0.12	0.02 $\pm$ 0.01	1
42.65 $\pm$ 0.02	0.60 $\pm$ 0.12	0.03 $\pm$ 0.02	1
43.13 $\pm$ 0.02	0.95 $\pm$ 0.12	0.06 $\pm$ 0.02	1
43.53 $\pm$ 0.01	1.20 $\pm$ 0.16	0.03 $\pm$ 0.01	1
43.97 $\pm$ 0.01	0.52 $\pm$ 0.13	0.01 $\pm$ 0.01	1
44.88 $\pm$ 0.07	2.13 $\pm$ 0.15	0.38 $\pm$ 0.08	2
45.53 $\pm$ 0.06	0.81 $\pm$ 0.19	0.08 $\pm$ 0.05	0
46.06 $\pm$ 0.09	0.53 $\pm$ 0.13	0.10 $\pm$ 0.07	3
47.30 $\pm$ 0.01	0.70 $\pm$ 0.13	0.02 $\pm$ 0.01	1
47.83 $\pm$ 0.03	0.76 $\pm$ 0.12	0.05 $\pm$ 0.03	1
48.36 $\pm$ 0.04	0.56 $\pm$ 0.13	0.07 $\pm$ 0.05	1
48.98 $\pm$ 0.11	0.81 $\pm$ 0.18	0.24 $\pm$ 0.16	2
49.71 $\pm$ 0.07	0.74 $\pm$ 0.16	0.15 $\pm$ 0.11	0
53.03 $\pm$ 0.17	0.91 $\pm$ 0.19	0.38 $\pm$ 0.24	2